Acta Cryst. (1994). B50, 695–703

Structure of Suberic Acid at 18.4, 75 and 123 K from Neutron Diffraction Data

BY QI GAO,* H.-P. WEBER† AND B. M. CRAVEN‡

Department of Crystallography, University of Pittsburgh, Pittsburgh, PA 15260, *USA*

AND R. K. MCMULLAN

Chemistry Department, Brookhaven National Laboratory, Upton, NY 11973, *USA*

(*Received* 22 *November* 1993; *accepted* 5 *April* 1994)

Abstract

Neutron diffraction data for suberic acid [$HOOC(CH_2)_6COOH$] were collected at 18.4, 75 and 123 K using a twinned crystal. The neutron data reduction included derivation of a complete set of corrected intensities, as if from a single crystal. This was followed by full-matrix structure refinement in the usual way. The molecule has an almost fully extended conformation with the hydrocarbon chains packed in an orthorhombic mode. Molecules form infinite hydrogen-bonded chains with crystallographic inversion centers occuring at the center and at the ends of each molecule. We suggest that at the twin boundary the hydrogen bonding is different, involving only the hydroxyl groups as both donors and acceptors. Accurate bond lengths have been obtained with corrections for thermal vibration (harmonic for C—C, C—O; harmonic and anharmonic for C—H). Values at the three temperatures agree well in terms of their e.s.d.'s (0.001 Å for C—C and C—O and 0.005 Å for C—H). Similar agreement is obtained for the corrected bond angles (e.s.d.'s 0.1° for C—C—C, 0.2° for H—C—H). For the methylene groups, the observed m.s. displacement parameters at each temperature are significantly greater at the middle of the molecule than at the ends. This indicates that the molecular backbone is vibrating internally. The thermal vibrations of the molecule have been analysed in terms of a simple segmented body model.

Introduction

Suberic acid [$HOOC(CH_2)_6COOH$] (Fig. 1) is a fatty acid that is well suited for a detailed crystallographic study. First, the chain is of sufficient length to establish a fatty acid character. Thus, the central methylene groups have methylene groups on each side as both first and second neighbors. Second, being a dicarboxylic acid, the molecule is hydrogen bonded at both ends, thereby reducing the m.s. amplitudes of thermal vibration and allowing the atomic positions and m.s. displacements to be accurately determined. Third, the molecule crystallizes in a centrosymmetric space group so that there are no ambiguities in phasing the structure factors. Fourth, the molecule lies on a crystallographic inversion center so that the asymmetric unit consists only of a half molecule. After we began our study, we discovered a disadvantage. All the crystals large enough for neutron diffraction were found to be twinned. However, we believe that the neutron diffraction

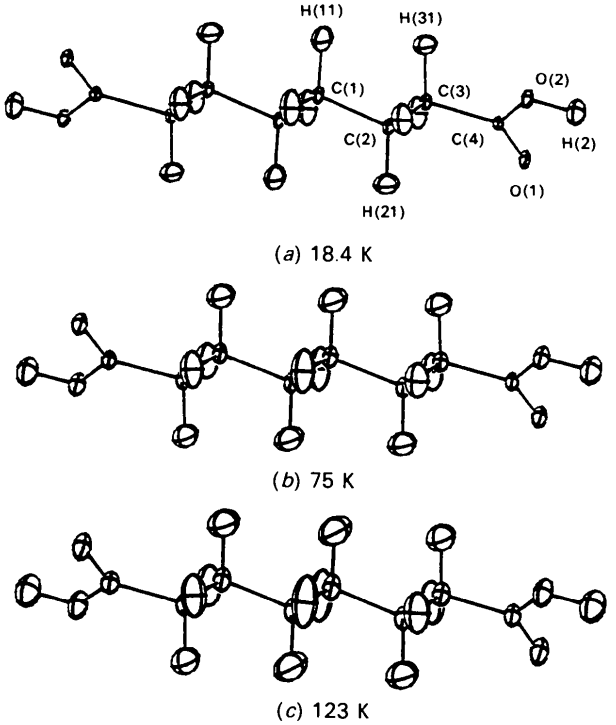

Fig. 1. Atomic nomenclature and 50% probability thermal ellipsoids (Johnson, 1976) for suberic acid.

* Present address: Bristol-Myers Squibb Pharmaceutical Research Institute, Wallingford, CT 06492, USA.

† Present address: Institute de Cristallographie, Université de Lausanne, BSP Dorigny, CH-1015 Lausanne, Switzerland.

‡ Author for correspondence.

data have been analysed in a way which overcomes this problem.

The crystal structure of suberic acid was first determined by Housty & Hospital (1964, 1965) using X-ray diffraction data collected at room temperature. The space group is $P2_1/c$ with two molecules in the unit cell. We found no phase transition when the crystal was cooled to 18.4 K.

Experimental

Suberic acid from Sigma Chemical Co. was dissolved in hot formic acid and crystallized at room temperature. The crystal (0.70 × 1.0 × 2.9 mm) used for neutron data collection was twinned, as were all other crystals of similar size. Efforts to obtain a large fragment by crystal cleavage or fracture were unsuccessful. The crystals were elongated on **c**, with prominent {100} and with (010) cleavage. A reentrant angle of *ca* 169° was observed between the twin components. This is near the value $180° - 2\beta = 164°$ obtained by X-ray diffraction. Precession X-ray photographs showed the twin plane to be (100), so that the components *A* and *B* have $\mathbf{a}^*_A = \mathbf{a}^*_B$ and $\mathbf{b}^*_A = -\mathbf{b}^*_B$ and the components have a common *hk*0 net. Planes in reciprocal space with a given *k* show duplicated lattice points in rows parallel to **a*** with near overlap at 18.4 K, when $l = 6, 7, 12, 13$.† A somewhat different overlap occurs at the other temperatures.

The neutron data were collected on a four-circle diffractometer with a Be(002) monochromator at the Brookhaven High Flux Beam Reactor. The wavelength of the neutron beam was 1.0499 Å, based on calibration with KBr ($a_o = 6.6000$ Å at 298 K). The twinned crystal was glued on a hollow aluminium pin, which was fastened at the bottom of an aluminium can filled with helium gas and the can was attached to the cold tip of a closed-cycle refrigerator,‡ which was then mounted onto the four-circle diffractometer. The crystal temperature was maintained within 0.5° of preset values.

Most measurements were made with crystal component *A*, which comprised the larger part of the twin. Well-resolved reflections from *A* were used to obtain the orientation matrix. The $\mathbf{c}^*_A$-axis was found to be 15° from the diffractometer φ-axis. The unit-cell parameters were measured at five temperatures in the range 18.4–123 K (Table 1), by least-squares fitting to observed $\sin^2\theta$ values for 32 accurately centered reflections in the range $51.1 < 2\theta < 57.1°$. The intensity data for *A* were collected in the range $-12 \rightarrow 12$ for *h*, $-7 \rightarrow 0$ for *k* and $0 \rightarrow 14$ for *l*, using $\theta/2\theta$ step scans. For reflections with $\sin\theta/\lambda < 0.44$ Å^{-1}, the scans were of constant width, $\Delta 2\theta = 1.785°$. For $0.44 < \sin\theta/\lambda < 0.78$ Å^{-1}, scan widths were given by $\Delta 2\theta = (2.68 + 1.824\tan\theta)°$. Intensity profiles were examined individually in order to estimate appropriate backgrounds for partially resolved *A* and *B* reflections. For completely resolved reflections, backgrounds were assumed to consist of the first and last tenth parts of the scan. The intensities were corrected for neutron absorption by an analytical procedure (de Meulenaer & Tompa, 1965; Templeton & Templeton, 1973). The linear absorption coefficient ($\mu = 0.296$ mm^{-1}) was calculated assuming the mass absorption coefficient of hydrogen to be $(10.055 + 14.117\lambda) = 24.864$ m^2 kg^{-1} (Koetzle & McMullan, 1980). In order to determine the relative contributions from the *A* and *B* components, the intensities of the resolved reflections 802, 604, $\bar{7}\bar{1}3$, $\bar{5}32$, $\bar{7}02$ 224 and 422 were measured for component *B*. This gave the average *A*:*B* ratio 1:0.174. The reciprocal lattices for *A* and *B* were transformed to a common Cartesian system in order to calculate ΔS, the separation of almost overlapping reflections. If $(\Delta S/|a^*|) < 0.08$, a pair of corrected intensities were obtained using equations such as

$$I(106) = \epsilon(106) + 0.174\epsilon(20\bar{6})$$

and

$$I(206) = 0.174\epsilon(106) + \epsilon(20\bar{6}),$$

where $I(hkl)$ is the measured intensity and $\epsilon(hkl)$ is the required intensity for an untwinned crystal of the same volume as component *A*. In the 18.4 K data set, 282 pairs of reflections were corrected, in the 75 K set 307 pairs and in the 123 K set 305 pairs. Further details of the data reduction procedure are given by Gao (1988). The total numbers of independent reflections were 1701, 1713 and 1718 at 18.4, 75 and 123 K, respectively. All reflections were included in the structure refinement.

The structure refinement began with the atomic positional and isotropic thermal parameters reported by Housty & Hospital (1965). Refinement was by full-matrix least squares using the program *NOOT* (Craven & Weber, 1986). The function minimized was $\sum w(F_o^2 - F_c^2)^2$ with weights $w = 1/\sigma^2(F_o^2)$ and $\sigma^2(F_o^2) = \sigma^2_{\text{counts}} + (0.015F_o^2)^2$. Neutron coherent

Table 1. *Crystal lattice parameters for suberic acid**

Temperature (K)	*a* (Å)	*b* (Å)	*c* (Å)	β (Å)	*V* (Å)
18.4	8.710 (1)	5.0885 (7)	9.815 (1)	95.07 (1)	433.3 (1)
50	8.723 (1)	5.0861 (7)	9.831 (2)	95.25 (2)	434.3 (1)
75	8.742 (2)	5.0841 (9)	9.850 (2)	95.43 (2)	435.8 (2)
100	8.761 (1)	5.0792 (5)	9.871 (1)	95.69 (1)	437.1 (1)
123	8.784 (2)	5.0721 (9)	9.889 (2)	95.95 (2)	438.2 (2)
298†	8.98	5.06	10.12	97.85	455.5

* Within the range 18.4–123 K, the unit-cell volume can be fitted within one e.s.d. using the polynomial $V = 432.71 + 0.026340T + 0.000166T^2$.

† X-ray data from Housty & Hospital (1965).

† See deposition footnote.

‡ Displex model CS-202.

Table 2. *Nuclear positional parameters* ($\times 10^4$) *and* U_{eq}'s ($Å^2 \times 10^4$)

The estimated standard deviations given in parentheses refer to the least-significant digit. For each atom the top line is for 18.4 K, the middle line is for 75 K and the bottom line is for 123 K. U_{eq}'s are defined by the expression $U_{eq} = \frac{1}{3}(U_{11} + U_{22} + U_{33} + 2U_{13}\cos\beta)$.

	x	y	z	U_{eq}
C(1)	690 (1)	852 (1)	242 (1)	82 (2)
	682 (1)	862 (1)	246 (1)	138 (2)
	667 (1)	876 (2)	255 (1)	205 (3)
C(2)	1438 (1)	65 (1)	1647 (1)	76 (2)
	1445 (1)	63 (1)	1642 (1)	128 (2)
	1450 (1)	57 (2)	1636 (1)	188 (3)
C(3)	2793 (1)	1846 (1)	2102 (1)	71 (2)
	2790 (1)	1848 (1)	2105 (1)	120 (2)
	2787 (1)	1860 (2)	2109 (1)	177 (3)
C(4)	3710 (1)	989 (1)	3395 (1)	64 (2)
	3711 (1)	995 (1)	3395 (1)	112 (2)
	3711 (1)	1000 (1)	3395 (1)	165 (3)
O(1)	3395 (1)	−943 (1)	4063 (1)	87 (2)
	3400 (1)	−945 (2)	4057 (1)	147 (3)
	3405 (1)	−950 (2)	4046 (1)	222 (4)
O(2)	4894 (1)	2549 (1)	3743 (1)	89 (2)
	4890 (1)	2550 (2)	3750 (1)	154 (3)
	4877 (1)	2555 (2)	3757 (1)	235 (4)
H(11)	1558 (2)	707 (4)	−503 (1)	281 (6)
	1541 (2)	770 (5)	−494 (2)	393 (8)
	1517 (3)	842 (6)	−486 (2)	553 (13)
H(12)	326 (2)	2922 (3)	264 (2)	277 (6)
	309 (2)	2915 (3)	277 (2)	398 (9)
	279 (3)	2910 (4)	304 (3)	553 (12)
H(21)	583 (2)	122 (3)	2410 (1)	253 (6)
	596 (2)	94 (4)	2404 (2)	335 (7)
	626 (2)	44 (5)	2394 (2)	443 (10)
H(22)	1842 (2)	−1974 (3)	1615 (2)	248 (6)
	1854 (2)	−1966 (3)	1597 (2)	322 (7)
	1872 (2)	−1962 (4)	1578 (2)	427 (9)
H(31)	3612 (2)	1950 (3)	1315 (1)	231 (6)
	3602 (2)	1968 (4)	1323 (2)	301 (7)
	3595 (2)	1995 (5)	1335 (2)	385 (9)
H(32)	2422 (2)	3880 (3)	2259 (2)	241 (6)
	2418 (2)	3883 (3)	2264 (2)	308 (6)
	2405 (2)	3884 (4)	2268 (2)	409 (9)
H(2)	5509 (1)	1890 (3)	4594 (1)	200 (6)
	5503 (2)	1895 (3)	4598 (1)	262 (6)
	5497 (2)	1914 (4)	4610 (2)	349 (8)

Table 3. *Nuclear anisotropic displacement parameters* ($Å^2 \times 10^4$)

Estimated standard deviations given in parentheses refer to the least-significant digit. For each atom the top line is for 18.4 K, the middle line is for 75 K and the bottom line is for 123 K. Anisotropic temperature factors are defined by the expression $T = \exp(-2\pi^2\sum_i\sum_j h_i h_j a^*_i a^*_j U_{ij})$.

	U_{11}	U_{22}	U_{33}	U_{12}	U_{13}	U_{23}
C(1)	80 (2)	86 (2)	75 (2)	−16 (2)	−23 (1)	12 (2)
	139 (2)	144 (3)	122 (2)	−18 (2)	−35 (2)	29 (2)
	206 (3)	207 (3)	187 (3)	−30 (3)	−55 (2)	54 (3)
C(2)	74 (2)	77 (2)	74 (2)	−8 (2)	−18 (2)	12 (2)
	126 (2)	131 (2)	118 (2)	−6 (2)	−25 (2)	27 (2)
	183 (3)	199 (3)	169 (3)	−11 (3)	−36 (3)	40 (3)
C(3)	69 (2)	70 (2)	71 (2)	−4 (2)	−17 (1)	9 (2)
	120 (2)	121 (2)	115 (2)	−3 (2)	−19 (2)	17 (2)
	179 (3)	179 (3)	164 (3)	−6 (3)	−30 (2)	31 (3)
C(4)	64 (2)	66 (2)	62 (2)	1 (2)	−6 (1)	8 (2)
	107 (2)	120 (2)	104 (2)	2 (2)	−13 (2)	18 (2)
	160 (3)	174 (3)	153 (3)	−6 (3)	−24 (2)	27 (3)
O(1)	88 (2)	87 (2)	82 (2)	−16 (2)	−21 (2)	30 (2)
	144 (3)	154 (3)	134 (3)	−24 (3)	−30 (2)	47 (3)
	215 (4)	232 (5)	203 (4)	−45 (4)	−58 (3)	82 (4)
O(2)	87 (2)	89 (2)	86 (2)	−27 (2)	−20 (2)	24 (2)
	157 (3)	153 (3)	141 (3)	−42 (2)	−38 (2)	41 (2)
	231 (4)	241 (4)	215 (4)	−72 (3)	−67 (3)	58 (3)
H(11)	202 (5)	474 (9)	171 (5)	−61 (6)	36 (4)	16 (6)
	280 (7)	677 (13)	224 (6)	−122 (8)	43 (5)	48 (7)
	382 (10)	990 (21)	282 (8)	−213 (12)	30 (7)	92 (11)
H(12)	336 (7)	135 (6)	334 (7)	20 (5)	−116 (6)	15 (5)
	492 (10)	192 (7)	462 (10)	11 (7)	−204 (8)	28 (7)
	723 (16)	249 (9)	605 (14)	44 (9)	−325 (12)	23 (9)
H(21)	199 (5)	381 (8)	185 (5)	−65 (5)	48 (4)	8 (5)
	261 (6)	521 (10)	228 (6)	−78 (7)	49 (5)	23 (7)
	345 (8)	694 (15)	294 (8)	−110 (9)	53 (7)	58 (9)
H(22)	281 (6)	140 (5)	306 (6)	20 (5)	−75 (5)	13 (5)
	361 (7)	173 (6)	403 (8)	21 (6)	−109 (6)	30 (6)
	452 (10)	257 (8)	527 (11)	29 (8)	−173 (9)	26 (8)
H(31)	186 (5)	344 (7)	170 (5)	−47 (5)	49 (4)	32 (5)
	247 (6)	444 (9)	214 (6)	−60 (6)	37 (5)	49 (6)
	302 (7)	581 (13)	273 (8)	−71 (8)	39 (6)	72 (8)
H(32)	284 (6)	129 (5)	296 (6)	35 (5)	−58 (5)	−7 (5)
	373 (7)	184 (6)	348 (7)	40 (6)	−65 (6)	1 (6)
	477 (10)	241 (8)	472 (10)	50 (8)	−121 (9)	5 (8)
H(2)	184 (5)	217 (5)	187 (5)	−25 (4)	−51 (4)	32 (4)
	244 (6)	302 (7)	225 (6)	−47 (5)	−59 (5)	48 (5)
	339 (8)	374 (9)	313 (8)	−80 (7)	−64 (6)	56 (7)

scattering lengths were taken from Koester (1977). The variables were the nuclear positional and anisotropic thermal displacement parameters and an isotropic extinction parameter for a crystal of type I with Lorentzian mosaicity (Becker & Coppens, 1974). Extinction effects were not severe [g = 18 (1), 21 (1) and 22 (1) $\times 10^{-4}$ rad^{-1} at 18.4, 75 and 123 K], the reflection most affected being $\bar{2}02$ with $0.763F_c^2$. The overall scale factor was not significantly different at the three temperatures [5.20 (4), 5.25 (4) and 5.20 (5) at 18.4, 75 and 123 K]. Refinements with a total of 119 variables gave $R_w(F^2) = 0.040$, 0.047 and 0.056 and goodness-of-fit 1.097, 1.008 and 1.002 for the data sets at 18.4, 75 and 123 K, respectively.* Final nuclear positional and anisotropic thermal parameters are in Tables 2 and 3.* In the final difference Fourier syntheses, the only possibly significant feature was a 4.9σ peak in the H(2)···O(1′) hydrogen bond, which occurred in the map for 123 K.

* Refinement with the data uncorrected for twinning gave $wR(F^2) = 0.080$, 0.099 and 0.086 at 18.4, 75 and 123 K.

Discussion

Crystal packing and molecular structure†

The crystal packing for suberic acid is very similar over the temperature range 18–298 K. As shown in Fig. 2(*a*), the molecules are hydrogen bonded to

* Tables of reflection data and a figure showing twinning in the *h*0*l* net plane have been deposited with the IUCr (Reference: BK0004). Copies may be obtained through The Managing Editor, International Union of Crystallography, 5 Abbey Square, Chester CH1 2HU, England.

† Molecular parameter values that are given in groups of three are values for the temperatures 18.4, 75 and 123 K, respectively.

form infinite chains along [101]. There are crystallographic inversion centers at the center of each molecule and at the ends, where there are pairs of hydrogen bonds. The hydrogen-bond distances and angles are not unusual [H(2)···O(1)′ distances 1.631 (1), 1.633 (2) and 1.634 (2) Å; O(2)—H(2)···O(1)′ angles 176.0 (1), 176.0 (1) and 176.5 (2)°]. At the twin boundary parallel to (100), we postulate the structure shown in Fig. 2(*b*). We assume that the boundary occurs at the plane $x = \frac{1}{2}$, with twin component *B* related to *A* by rotation of 180° about the common **a*** axis. A translation of *B* then allows the formation of a new set of hydrogen bonds, which involves only the hydroxyl group O(2)—H(2) as both donor and acceptor.

The projection down [101] in Fig. 3 shows the orthorhombic packing mode for the hydrocarbon chains (Segerman, 1965; Shipley, 1986). The dihedral angle between (010) and the plane of the chain zigzag changes only slightly with temperature (51.8, 52.5 and 53.6°). The shortest chain–chain distance (2.24, 2.24 and 2.24 Å) is between H(12) and H(12) at $(-x, 1-y, -z)$.

The molecules are almost in a fully extended conformation so that the six tetrahedral C atoms are almost coplanar. When the best least-squares plane through these atoms is written $Px + Qy + Rz = 0$, then $P = -5.699$, -5.769 and -5.872 Å, $Q = 3.145$, 3.091 and 3.007 Å and $R = 4.828$, 4.942 and 5.104 Å, and the greatest nuclear displacement from the plane is for the central C(1) [−0.009 (1), −0.005 (1) and −0.002 (1) Å]. The plane of the carboxylate group is slightly twisted from the plane of the chain zigzag, as indicated by the dihedral angles 6.42 (7), 5.98 (9) and 5.29 (11)° and by the C(1)—C(2)—C(3)—C(4) bond torsion angles (see Table 4).

In Table 4, bond lengths and angles are given before and after correction for thermal vibration effects. The corrections are small, but for most bond lengths they are significant in terms of the e.s.d.'s in the corrected distances, which are 0.001 Å for C—C and C—O bond lengths and 0.005 Å for C—H bond lengths. For each C—C and C—O bond length, uncorrected values tend to decrease with increasing temperature, the differences being most notable for C(1′)—C(1) (1.524, 1.522 and 1.515 Å) and C(4)—O(2) (1.322, 1.320 and 1.313 Å). This is consistent with thermal librational effects. After correction for harmonic thermal libration, the three values are in better agreement (1.525, 1.524 and 1.519, and 1.324, 1.323 and 1.318 Å, respectively).

Average corrected values for the three distinct bonds involving tetrahedrally coordinated C atoms are also in close agreement, although the corrected C(2)—C(3) bond length (1.523 Å) may be slightly shorter than the others (1.526 Å). These values agree well with those obtained for propane using microwave spectroscopy [1.526 (2) Å; Lide, 1960] and cor-

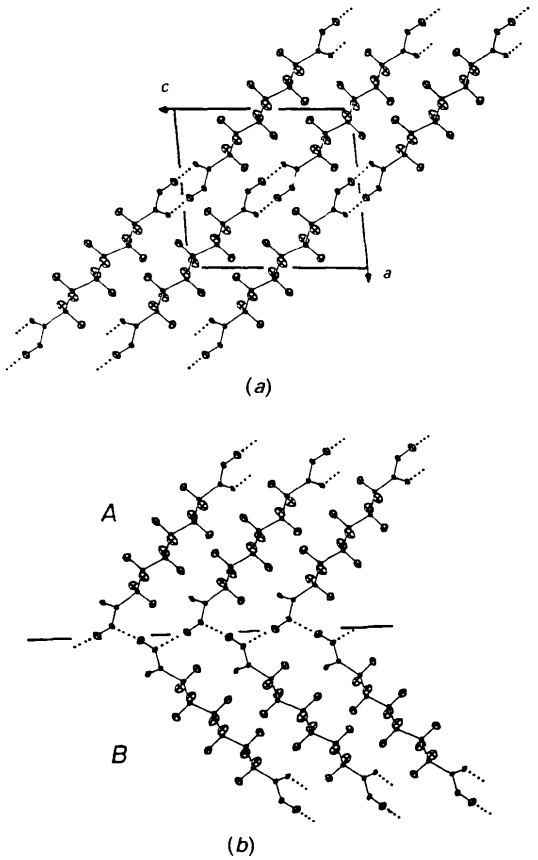

Fig. 2. Molecular packing and hydrogen bonding in projection down *b*. The hydrogen bonds are shown as dotted lines. (*a*) The crystal structure and the unit cell. (*b*) Proposed structure at the boundary between twin components *A* and *B*. Component *A* is the same as in the upper half of (*a*) above. Component *B* is from the lower half of (*a*) after 180° rotation in the twin plane.

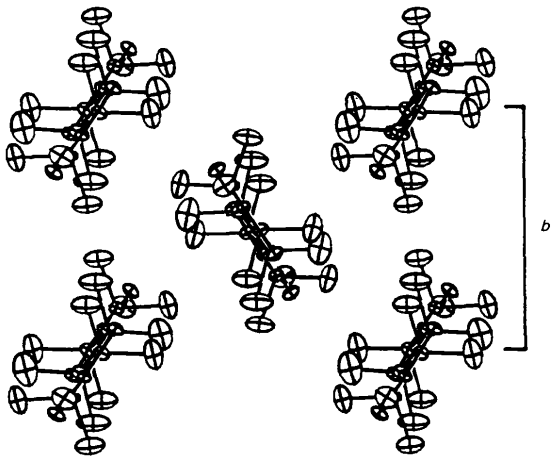

Fig. 3. Crystal structure of suberic acid in projection down [101], showing the orthorhombic packing of the chains.

Table 4. *Internuclear distances* (Å) *and angles* (°) *in suberic acid*

(*a*) Bond lengths

First line: values uncorrected for thermal motion; second line: values corrected for harmonic librational motion; third line: values corrected for harmonic libration and anharmonic bond stretching. The intermolecular O(1′)···H(2) distances are uncorrected.

	Temperature (K)				Temperature (K)		
	18.4	75	123		18.4	75	123
C(1′)—C(1)	1.524 (1)	1.522 (1)	1.515 (1)	C(2)—H(21)	1.102 (2)	1.104 (2)	1.095 (2)
	1.525 (1)	1.524 (1)	1.519 (1)		1.105 (2)	1.109 (3)	1.103 (3)
C(1)—C(2)	1.526 (1)	1.525 (1)	1.522 (1)		1.087 (2)	1.093 (3)	1.085 (4)
	1.527 (1)	1.527 (1)	1.525 (1)	C(2)—H(22)	1.097 (2)	1.094 (2)	1.093 (2)
C(2)—C(3)	1.523 (1)	1.521 (1)	1.523 (1)		1.100 (2)	1.099 (3)	1.101 (3)
	1.525 (1)	1.524 (1)	1.530 (1)		1.081 (2)	1.083 (3)	1.081 (4)
C(3)—C(4)	1.503 (1)	1.502 (1)	1.501 (1)	C(3)—H(31)	1.098 (2)	1.097 (2)	1.099 (2)
	1.504 (1)	1.504 (1)	1.504 (1)		1.101 (3)	1.102 (3)	1.107 (3)
C(4)—O(1)	1.226 (1)	1.227 (1)	1.225 (1)		1.079 (4)	1.086 (5)	1.094 (5)
	1.229 (1)	1.232 (1)	1.234 (1)	C(3)—H(32)	1.099 (2)	1.100 (2)	1.096 (2)
C(4)—O(2)	1.322 (1)	1.320 (1)	1.313 (1)		1.102 (3)	1.105 (3)	1.105 (3)
	1.324 (1)	1.323 (1)	1.318 (1)		1.086 (4)	1.086 (5)	1.086 (5)
C(1)—H(11)	1.100 (2)	1.096 (2)	1.099 (2)	O(2)—H(2)	1.009 (1)	1.005 (2)	1.009 (2)
	1.102 (2)	1.100 (3)	1.107 (3)		1.012 (3)	1.011 (3)	1.018 (4)
	1.083 (4)	1.083 (5)	1.087 (5)		0.991 (4)	0.990 (4)	0.987 (5)
C(1)—H(12)	1.101 (2)	1.095 (2)	1.089 (2)	O(1′)···H(2)	1.631 (1)	1.633 (2)	1.634 (2)
	1.103 (2)	1.099 (3)	1.097 (3)				
	1.088 (4)	1.079 (5)	1.080 (5)				

(*b*) Bond angles

First line: values uncorrected for thermal motion; second line: values corrected for thermal motion.

	Temperature (K)				Temperature (K)		
	18.4	75	123		18.4	75	123
C(1′)—C(1)—C(2)	113.2 (1)	113.4 (1)	113.6 (1)	C(1)—C(2)—H(21)	110.3 (1)	110.1 (1)	110.3 (1)
	113.2 (1)	113.0 (1)	113.1 (1)		110.3 (1)	110.2 (1)	110.4 (2)
C(1)—C(2)—C(3)	111.5 (1)	111.8 (1)	112.0 (1)	C(1)—C(2)—H(22)	109.6 (1)	109.4 (1)	109.5 (1)
	111.3 (1)	111.4 (1)	111.4 (1)		109.6 (1)	109.4 (1)	109.5 (2)
C(2)—C(3)—C(4)	114.5 (1)	114.8 (1)	114.7 (1)	H(21)—C(2)—C(3)	109.7 (1)	109.8 (1)	109.7 (1)
	114.3 (1)	114.4 (1)	114.1 (1)		109.8 (1)	109.9 (1)	109.9 (2)
C(3)—C(4)—O(1)	123.8 (1)	123.6 (1)	123.4 (1)	H(22)—C(2)—C(3)	109.2 (1)	109.2 (1)	108.9 (1)
	123.9 (1)	123.7 (1)	123.6 (1)		109.3 (1)	109.3 (1)	109.1 (2)
C(3)—C(4)—O(2)	112.8 (1)	113.2 (1)	113.2 (1)	H(21)—C(2)—H(22)	106.3 (1)	106.5 (1)	106.4 (2)
	112.6 (1)	112.9 (1)	112.7 (1)		106.4 (2)	106.6 (2)	106.5 (2)
O(1)—C(4)—O(2)	123.3 (1)	123.2 (1)	123.3 (1)	C(2)—C(3)—H(31)	110.9 (1)	110.8 (1)	110.9 (1)
	123.5 (1)	123.5 (1)	123.8 (1)		111.1 (1)	110.9 (1)	111.1 (2)
C(1′)—C(1)—H(11)	108.9 (1)	109.2 (1)	108.9 (2)	C(2)—C(3)—H(32)	111.8 (1)	111.9 (1)	111.6 (1)
	108.9 (1)	109.3 (1)	109.1 (2)		111.8 (1)	112.0 (1)	111.7 (2)
C(1′)—C(1)—H(12)	109.3 (1)	109.4 (1)	109.6 (2)	H(31)—C(3)—C(4)	106.2 (1)	106.2 (1)	106.1 (1)
	109.4 (1)	109.5 (1)	109.8 (2)		106.2 (1)	106.3 (1)	106.1 (2)
H(11)—C(1)—C(2)	108.6 (1)	108.6 (1)	108.6 (2)	H(32)—C(3)—C(4)	107.2 (1)	107.0 (1)	107.3 (1)
	108.7 (1)	108.7 (1)	108.7 (2)		107.2 (1)	107.1 (1)	107.5 (2)
H(12)—C(1)—C(2)	109.5 (1)	109.6 (1)	109.5 (1)	H(31)—C(3)—H(32)	105.7 (1)	105.5 (1)	105.7 (2)
	109.6 (1)	109.6 (1)	109.5 (2)		105.7 (2)	105.5 (2)	105.7 (2)
H(11)—C(1)—H(12)	107.1 (1)	106.5 (2)	106.4 (2)	C(4)—O(2)—H(2)	111.1 (1)	111.3 (1)	111.9 (1)
	107.1 (2)	106.6 (2)	106.4 (2)		110.9 (1)	111.0 (1)	111.3 (2)

(*c*) Bond torsion angles

	Temperature (K)				Temperature (K)		
	18.4	75	123		18.4	75	123
C(2′)—C(1′)—C(1)—C(2)	180	180	180	H(12)—C(1)—C(2)—H(22)	−177.78 (12)	−177.93 (15)	−178.18 (19)
C(1′)—C(1)—C(2)—C(3)	−179.00 (4)	−179.36 (5)	−179.78 (7)	H(21)—C(2)—C(3)—H(31)	−175.16 (12)	−175.45 (14)	−176.62 (18)
C(1)—C(2)—C(3)—C(4)	−172.75 (4)	−173.25 (5)	−173.96 (7)	H(21)—C(2)—C(3)—H(32)	−57.46 (13)	−57.98 (15)	−59.02 (20)
C(2)—C(3)—C(4)—O(1)	−1.59 (8)	−1.74 (9)	−1.97 (12)	H(22)—C(2)—C(3)—H(31)	68.59 (13)	68.16 (15)	67.32 (19)
C(2)—C(3)—C(4)—O(2)	178.69 (5)	178.47 (6)	178.35 (8)	H(22)—C(2)—C(3)—H(32)	−173.70 (12)	−174.37 (14)	−175.08 (18)
H(11)—C(1)—C(2)—H(21)	−177.95 (13)	−178.68 (15)	−179.17 (20)	C(3)—C(4)—O(2)—H(2)	−177.96 (9)	−178.10 (11)	−178.54 (14)
H(11)—C(1)—C(2)—H(22)	−61.16 (13)	−61.97 (16)	−62.44 (20)	O(1)—C(4)—O(2)—H(2)	2.32 (12)	2.11 (14)	1.78 (18)
H(12)—C(1)—C(2)—H(21)	65.43 (13)	65.37 (16)	65.10 (21)				

rected values obtained for γ-aminobutyric acid from neutron diffraction [1.525 (1) and 1.528 (1) Å; Weber, Craven & McMullan (1983)]. In suberic acid, the C(3)—C(4) bond, which involves a trigonal carbon, is significantly shorter (average corrected value 1.504 Å), being in agreement with the corresponding bond length obtained for succinic acid from a low-temperature (77 K) neutron diffraction study [1.503 (2) Å after correction for rigid body libration; Levial, Auvert & Savariault (1981)]. It is of interest to note that whereas the C—C bond involving the carboxylic acid group is shorter than the chain C—C bonds, when this bond involves a charged carboxylate group it becomes longer [1.534 (1) Å in γ-aminobutyric acid; Weber, Craven & McMullan, 1983].

Table 5. *Relative m.s. nuclear displacements* (Å^2) *along A—H bonds*

Values given are $\Delta(H,A) = \langle u^2_H \rangle - \langle u^2_A \rangle$, where $\langle u^2_H \rangle$ and $\langle u^2_A \rangle$ are m.s. displacements of H and *A* along the A—H bond direction.

Bond	18.4 K	75 K	123 K
C(1)—H(11)	0.0062 (6)	0.0057 (8)	0.0064 (12)
C(1)—H(12)	0.0050 (6)	0.0066 (8)	0.0057 (12)
C(2)—H(21)	0.0060 (6)	0.0055 (7)	0.0059 (9)
C(2)—H(22)	0.0064 (6)	0.0052 (6)	0.0066 (9)
C(3)—H(31)	0.0041 (5)	0.0055 (6)	0.0044 (9)
C(3)—H(32)	0.0055 (6)	0.0062 (6)	0.0063 (9)
O(2)—H(2)	0.0070 (5)	0.0069 (7)	0.0102 (9)

The C—H bond lengths have been corrected for harmonic librations and also for anharmonic stretching vibrations. The former correction is a lengthening and the latter a shortening. The average uncorrected value for all C—H bonds in suberic acid is 1.098 Å and the average corrected value is 1.085 Å, so that the net effect of the correction is a shortening of 0.013 Å.

Corresponding bond angles at the three temperatures are in good agreement (Table 4). Corresponding bond angles at the three distinct tetrahedral carbons are slightly different, as might be expected because of differences in their molecular environment. Thus, the C(1) methylene group is the only one that has two other methylenes as second-nearest neighbors along the chain. The bond-angle differences are small, but they are highly significant in terms of their e.s.d.'s. For example, after correction for thermal vibration, the C—C—C angles have average values of 113.1, 111.4 and 114.3 (1)° at C(1), C(2) and C(3), respectively. Averaging over all three tetrahedral C atoms gives corrected values 112.9° for C—C—C, 106.3° for H—C—H and 109.3° for C—C—H.

Molecular thermal vibrations

Plots of the equivalent isotropic m.s. displacement parameters U_{eq} (from Table 2) show the expected increase of U_{eq} with temperature (Fig. 4). The slight nonlinearity of these plots is attributed to zero-point vibration effects, which are expected to be of greater relative significance at 18.4 K. However, at least one additional data set collected at *ca* 30 K would be required in order to confirm this interpretation. As can be seen in Fig. 4, the m.s. nuclear displacements, other than those of oxygen, become progressively greater for the atoms towards the center of the chain. This indicates that the chains are vibrating non-rigidly.

Further evidence of nonrigid thermal vibrations of the H nuclei is obtained by applying the Hirshfeld test (Hirshfeld, 1976) to the C—H bonds. This consists of deriving $\Delta(H,A) = \langle u^2_H \rangle - \langle u^2_A \rangle$, which is the difference in m.s. amplitudes of nuclear displacement along the H—*A* bond direction. Calculations were made with computer programs by Craven & He (1982). As can be seen in Table 5, $\Delta(H,A)$ values are significantly nonzero for all C—H and O—H bonds at each temperature, indicating the observable contributions from bond-stretching vibrations. It is of interest that, except for O—H, values of $\Delta(H,A)$ are remarkably constant at all three temperatures, indicating that the population of energy levels for these vibrations is not significantly different over the range 18–123 K. Furthermore, values of $\Delta(H,C)$ are in good agreement with those obtained for methylene groups in cholesteryl acetate and several other crystal structures determined from neutron diffraction [see Table 6 in Weber, Craven, Sawzik & McMullan (1991)].

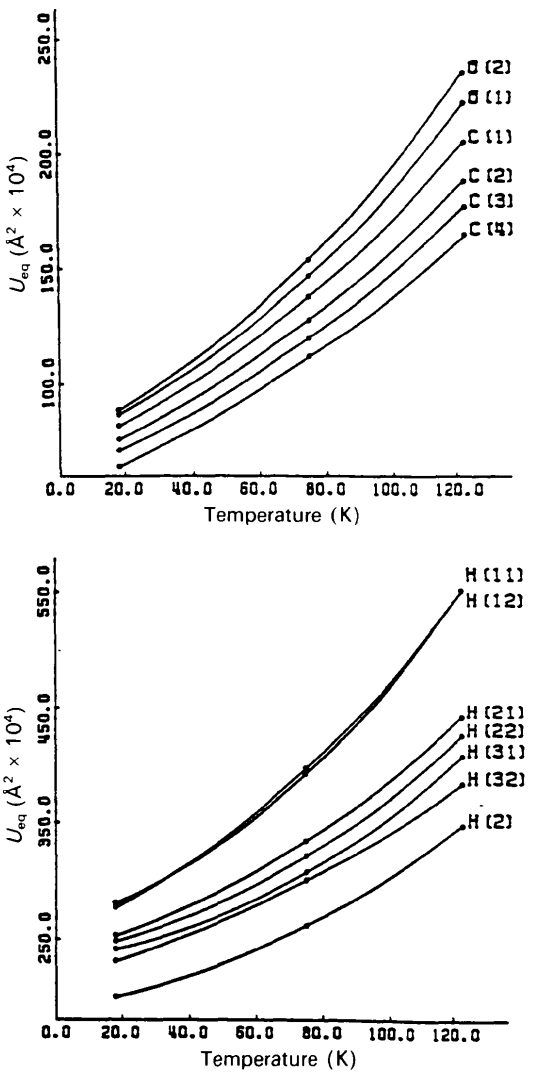

Fig. 4. Plots of U_{eq} (Å^2 × 10^4) *versus* temperature for each atomic nucleus. The curves are shown merely to connect points for the same nucleus and cannot be used for purposes of interpolation.

Corrections for anharmonic C—H and O—H bond stretching (Table 4) were applied using the empirical expression $\delta = -3a\Delta(\mathrm{H},A)/2$, where $a = 2.0$ Å^{-1} is derived from spectroscopic data and represents the asymmetry of the Morse potential function for the C—H and O—H groups (Kuchitsu & Bartell, 1961; Kuchitsu & Morino, 1965; Craven & Swaminathan, 1984).

In suberic acid, values of $\Delta(A,B)$ for other bonds and for intramolecular nonbonded atom pairs (Rosenfield, Trueblood & Dunitz, 1978) are small and only marginally significant; for example, 0.0011 (3) Å^2 for C(1)···O(2) and 0.0010 (3) Å^2 for C(3)···O(2). However, passing the nonrigidity test is not a sufficient requirement, because this test is insensitive to the internal vibrations of the chain in directions almost normal to the plane of the zigzag and normal to the interatomic vectors $A\cdots B$. As already noted, the suberic acid chains must be vibrating nonrigidly because, at each temperature, the methylene groups near the center of the molecule have larger m.s. displacements than those at the ends (Fig. 4).

As a benchmark, the analysis of the anisotropic nuclear m.s. displacements began by assuming the simple rigid-body model for the molecular vibrations (Schomaker & Trueblood, 1968). A least-squares fit was made using the program *EKRT* (He & Craven, 1993) in order to minimize the residual $\sum w\Delta^2$, where $w = \sigma^{-2}(U_{\mathrm{obs}})$ and $\Delta = (U_{\mathrm{obs}} - U_{\mathrm{calc}})$ and the sum is over the six components U_{ij} for each atom and over all atoms. With all atomic nuclei, including H, this gave $R_w(U) = [\sum w\Delta^2/\sum wU_{\mathrm{obs}}^2]^{1/2} = 0.37$, 0.30 and 0.27 for the three temperatures and goodness-of-fit $\mathrm{GOF} = [\sum w\Delta^2/(m-n)]^{1/2} = 11.8$, 12.0 and 10.8. The agreement is greatly improved when all the H nuclei are omitted [$wR(U) = 0.093$, 0.094 and 0.101]. However, without the H-atom nuclei and disregarding the carbonyl O(1), the other nuclei all lie close to two parallel straight lines. Under such circumstances, the least-squares normal equation matrix becomes almost singular (Johnson, 1970). For this reason, the methylene H nuclei were retained, but were assigned m.s. displacements corrected for the internal CH_2 vibrations. The corrections were assumed to be the same for all three temperatures and for all H-atom nuclei and were assigned values of 0.0060 Å^2 for the C—H stretching vibrations, 0.0243 Å^2 for the CH_2 in-plane vibrations and 0.0158 Å^2 for the CH_2 out-of-plane vibrations (Weber, Craven, Sawzik & McMullan, 1991). The rigid-body fit with inclusion of all H-atom nuclei except H(2) was then much improved, giving $wR(U) = 0.169$, 0.171 and 0.191 and GOF = 4.39, 6.44 and 7.67. With U_{ij} components transformed to molecular inertial axes (z along the molecular long axis, x almost normal to the plane of the zigzag chain, Fig. 5), it was found that the largest differences ($U_{\mathrm{obs}} - U_{\mathrm{calc}}$) involved U_{11}, that is, the m.s. nuclear displacements normal to the plane of the zigzag chain. Such differences were consistent with the presence of out-of-plane internal vibrations of the chain, which are not taken into account with the rigid-body model.

Analysis was continued using the segmented body model of He & Craven (1993). Initially, the molecule was assumed to consist of eight rigid segments, namely the six methylene groups and the two carboxylic acid groups with H(2) omitted as before. Internal torsional vibration was introduced about each of the seven C—C bonds of the chain. The model differs from that of Dunitz & White (1973) in that for each C—C bond torsion, the nuclear displacements are required to satisfy the Eckart conditions (Eckart, 1935), namely that each internal vibration makes no contribution to the overall angular and linear momentum of the molecule. Relative nuclear displacements consistent with the Eckart conditions are shown in Fig. 5 for torsion about the C(1)—C(2) and C(1)—C(1′) bonds in suberic acid. It should be noted that each internal torsional mode involves the displacement of *all* atomic nuclei in the molecule, including those which lie on the axis of torsion. Indeed for the C(1)—C(1′) torsional mode, it can be seen that C(1) and C(1′) have the largest displacements. It is also assumed that there is no interaction between any of the contributing vibrations. Thus, the total m.s. displacement for a given atom is obtained as the sum of m.s. displacements from the rigid-body motion together with the sum of m.s. angular displacements $\langle\varphi^2\rangle$ from each of the internal torsional vibrations. With the eight-segment

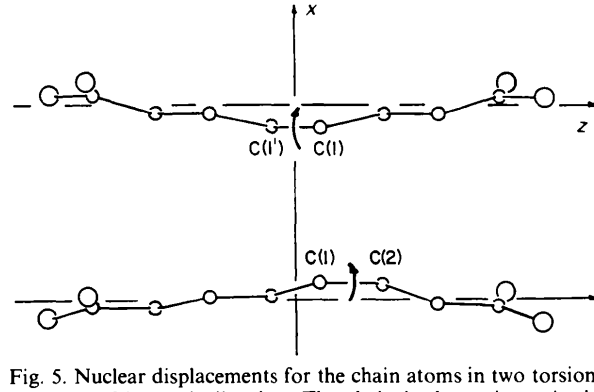

Fig. 5. Nuclear displacements for the chain atoms in two torsional modes of internal vibration. The chain is shown in projection down the molecular inertial y-axis. The inertial axes x and z are close to the normal to the zigzag plane of the chain and the molecular long axis, respectively. In projection, the mean positions of all nuclei are very close to the z-axis. Displacements along x are on an exaggerated scale. Above: torsion about the C(1′)—C(1) bond; below: torsion about the C(1)—C(2) bond. The symmetry-related torsional mode about the C(1′)—C(2′) bond was also incorporated in modeling the internal vibrations of suberic acid.

Table 6. *Segmented body thermal vibration analysis*

The molecule $[O_2C(CH_2)_2]$-$[CH_2]$-$[CH_2]$-$[(CH_2)_2CO_2]$ is assumed to vibrate as a body with four rigid segments as indicated by the square brackets. The hydroxyl H-atom nuclei are omitted and U_{ij} components for the other H atoms have standard corrections for the internal vibrations of the methylene groups (Weber, Craven, Sawzik & McMullan, 1991). The variables are the components of the overall rigid-body **T** and **L** tensors (Schomaker & Trueblood, 1968), referred to the molecular inertial axes and the center of mass as the origin and $\langle\varphi^2\rangle$, the m.s. displacements for the torsional libration about the C—C bonds that link the segments (Fig. 5). Because of the crystallographic inversion center, the rigid-body cross-tensor **S** = 0. It is assumed that there are no interactions among the rigid-body motion and the internal torsional motions (He & Craven, 1993).

Temperature (K)	18.4	75	123
$wR(U)$	0.117	0.111	0.126
Goodness-of-fit	3.03	4.19	5.05
T_{11} (Å^2 × 10^4)	80 (4)	123 (6)	173 (10)
T_{22}	66 (3)	115 (4)	167 (7)
T_{33}	54 (2)	93 (2)	134 (4)
T_{12}	9 (2)	13 (4)	17 (7)
T_{13}	5 (2)	−8 (2)	−13 (4)
T_{23}	3 (2)	13 (2)	19 (4)
L_{11}(deg^2)	0.0 (1)	−0.1 (1)	0.0 (1)
L_{22}	0.1 (1)	−0.1 (1)	0.0 (1)
L_{33}	8.8 (10)	16.3 (16)	30.2 (28)
L_{12}	0.1 (1)	0.1 (1)	0.2 (1)
L_{13}	0.1 (1)	0.2 (3)	0.3 (5)
L_{23}	0.0 (1)	−0.1 (2)	−0.3 (3)
$\langle\varphi^2\rangle$[C(2)—C(3)] (deg^2)	11.9 (17)	21 (3)	35 (5)
$\langle\varphi^2\rangle$[C(1)—C(1′)]	7.8 (15)	14 (2)	27 (4)

model, it was found that, at all three temperatures, only the torsions about the more centrally located bonds C(1)—C(1′) and C(1)—C(2) and the symmetry-related torsion C(1′)—C(2′) have m.s. librational amplitudes which are greater than 1.2σ. A model with C—C—C bond angle bending at each carbon was tested, but none of these bending vibrations were found to be significant. Accordingly, the methylene groups at C(3) and C(2) were fused to the carboxylic acid, giving a model with only four rigid segments and three internal bond torsions. The results from this model are summarized in Table 6, from which it can be seen that $wR(U) = 0.117$, 0.111 and 0.126, including all atoms except H(2). Also from Table 6 it can be seen that the rigid-body librational terms are insignificant, except for L_{33}, so that libration occurs only about directions close to the molecular long axis. The largest least-squares correlation for this model was −0.70 between T_{11} and L_{22}. Subsequently, we tested a model which included physical interaction between the internal torsions and the overall rigid-body motion (Dunitz, Schomaker & Trueblood, 1988; He & Craven, 1993). This involves the determination of additional variables such as $\langle\varphi t_x\rangle$ and $\langle\varphi\lambda_z\rangle$, where t_x and λ_z are Cartesian components of the rigid-body displacement. However, the fit with this model was unsatisfactory because an almost complete least-squares correlation developed between T_{11} and L_{22}. Harmonic librational corrections to the bond lengths and angles (Table 4) were derived from the model (Table 6) in which the interactions of internal and external vibrations are neglected.

The thermal vibrations in suberic acid have been analyzed in terms of a model which is greatly simplified when compared with a complete normal mode analysis for the *n*-paraffins (Schachtschneider & Snyder, 1963) or an extended polymethylene chain (Tasumi, Shimanouchi & Miyazawa, 1963). The normal mode approach is required in order to understand complex spectra which extend over a wide frequency range. Here we seek a fit to the experimentally determined nuclear m.s. displacements in terms of selected internal coordinates (Fig. 5), which are efficient for the purpose. The simple segmented body model does this reasonably well, with only two distinct torsional modes. Intuitively, these particular modes would seem to be important for suberic acid.

This work was supported by a grant HL-20350 from the National Institutes of Health. The neutron data were collected at Brookhaven National Laboratory under contract DE-AC02-76CH00016 from the US Department of Energy.

References

BECKER, P. J. & COPPENS, P. (1974). *Acta Cryst.* A**30**, 129–147.

CRAVEN, B. M. & HE, X. (1982). *Programs for Thermal Motion Analysis.* Technical Report, Department of Crystallography, Univ. of Pittsburgh, PA, USA.

CRAVEN, B. M. & SWAMINATHAN, S. (1984). *Trans. Am. Cryst. Assoc.* **20**, 133–135.

CRAVEN, B. M. & WEBER, H. P. (1986). *Program NOOT for Refinement with Neutron Diffraction Data.* Technical Report, Department of Crystallography, Univ. of Pittsburgh, PA, USA.

DUNITZ, J. D., SCHOMAKER, V. & TRUEBLOOD, K. N. (1988). *J. Phys. Chem.* **92**, 856–867.

DUNITZ, J. D. & WHITE, D. N. J. (1973). *Acta Cryst.* A**29**, 93–94.

ECKART, C. (1935). *Phys. Rev.* **47**, 552–558.

GAO, Q. (1988). PhD Dissertation, Univ. of Pittsburgh, PA, USA.

HE, X. M. & CRAVEN, B. M. (1993). *Acta Cryst.* A**49**, 10–22.

HIRSHFELD, F. L. (1976). *Acta Cryst.* A**32**, 239–244.

HOUSTY, P. J. & HOSPITAL, M. (1964). *Acta Cryst.* **17**, 1387–1390.

HOUSTY, P. J. & HOSPITAL, M. (1965). *Acta Cryst.* **18**, 753–755.

JOHNSON, C. K. (1970). In *Crystallographic Computing*, edited by F. R. AHMED, pp. 207–219. Copenhagen: Munksgaard.

JOHNSON, C. K. (1976). *ORTEP*II. Report ORNL-5318. Oak Ridge National Laboratory, Tennessee, USA.

KOESTER, L. (1977). *Neutron Physics*, edited by G. HOHLER, p. 1. Berlin: Springer.

KOETZLE, T. F. & MCMULLAN, R. K. (1980). *Research Memo C-4.* Brookhaven National Laboratory, USA.

KUCHITSU, K. & BARTELL, L. S. (1961). *J. Chem. Phys.* **35**, 1945–1949.

KUCHITSU, K. & MORINO, Y. (1965). *Bull. Chem. Soc. Jpn*, **38**, 805–813.

LEVIAL, J. L., AUVERT, G. & SAVARIAULT, J. M. (1981). *Acta Cryst.* B**37**, 2185–2189.

LIDE, D. R. (1960). *J. Chem. Phys.* **33**, 1514–1518.

MEULENAER, J. D. DE & TOMPA, H. (1965). *Acta Cryst.* **19**, 1014–1018.

ROSENFIELD, R. E., TRUEBLOOD, K. N. & DUNITZ, J. D. (1978). *Acta Cryst.* A**34**, 828–829.

SCHACHTSCHNEIDER, J. H. & SNYDER, R. G. (1963). *Spectrochim. Acta*, **19**, 117–168.
SCHOMAKER, V. & TRUEBLOOD, K. N. (1968). *Acta Cryst.* B**24**, 63–76.
SEGERMAN, E. (1965). *Acta Cryst.* **19**, 789–796.
SHIPLEY, G. G. (1986). In *The Handbook of Lipid Research* 4 (*The Physical Chemistry of Lipids*), edited by DONALD M. SMALL, Ch. 5. New York: Plenum Press.
TASUMI, M., SHIMANOUCHI, T. & MIYAZAWA, T. (1963). *J. Mol. Spectrosc.* **11**, 422–432.
TEMPLETON, L. K. & TEMPLETON, D. H. (1973). *Abstr. Am. Cryst. Assoc. Meeting*, p. 143. Storrs, CT, USA.
WEBER, H.-P., CRAVEN, B. M. & MCMULLAN, R. K. (1983). *Acta Cryst.* B**39**, 360–366.
WEBER, H.-P., CRAVEN, B. M., SAWZIK, P. & MCMULLAN, R. K. (1991). *Acta Cryst.* B**47**, 116–127.

Acta Cryst. (1994). B**50**, 703–707

Dimethylaminobenzonitrile: Structure of the Lower-Temperature Solid Phase. Comparison with the Structure of the Higher-Temperature Phase and Correlation with Optical Spectroscopic Properties

BY GEOFFREY B. JAMESON, BASHIR M. SHEIKH-ALI AND RICHARD G. WEISS

Department of Chemistry, Georgetown University, Washington, DC 20057, *USA*

(*Received* 30 *August* 1993; *accepted* 8 *March* 1994)

Abstract

The crystal and molecular structures of 4-(*N*,*N*′-dimethylamino)benzonitrile (DMABN), $C_9H_{10}N_2$, in its lower-temperature solid phase at 173 K are reported and compared with those in the higher-temperature solid phase at 301 K. The molecular packing arrangement is correlated with some optical spectroscopic properties of the crystal.

Introduction

The intriguing photophysical properties of dialkylaminobenzonitriles [typified by the classic example *p*-(*N*,*N*′-dimethylamino)benzonitrile (DMABN)] have been investigated for more than 30 years (Lippert, Lüder & Boos, 1962). This interest has largely been driven by attempts to understand the structural and electronic features of dimethylaminobenzonitriles (and other molecules), which exhibit dual fluorescence bands, presumably *via* interconversion of twisted intramolecular charge-transfer (TICT) and untwisted locally excited (LE) states (see scheme below) (Rotkiewicz, Grellmann & Grabowski, 1973; Siemiarczuk, Grabowski, Krowczynski, Asher & Ottolenghi, 1977). Surprisingly, and in spite of the acknowledged dependence of ground-state conformations and configurations on the nature of the emitting excited states (Rettig, 1988), only last year has the crystalline structure of DMABN been published (Gourdon *et al.*, 1993; Heine, Herbst-Irman, Stalke, Kuhnle & Zachariasse, 1994), and only in the higher-temperature solid phase.

Here, we report the structure and unit-cell packing of DMABN in its lower-temperature solid phase and compare these with those of the higher-temperature phase. We have also duplicated the reported higher-temperature phase results. Although there are surprisingly minor differences in the conformation of molecules in the two phases, the unit-cell dimensions are very different. Both the crystal structures and their modes of packing provide insights concerning the photophysical data, especially in the solid state.

Experimental

Monoclinic crystals, m.p. 348–349 K (ref. m.p. 346–348 K; Rotkiewicz, Leismann & Rettig, 1989), were prepared by slow evaporation of a solution of doubly-sublimed DMABN (Aldrich, 98%) in hexane/ether. A reversible phase transition (confirmed to be solid–solid by optical microscopy) was detected at 261.1 K ($\Delta H = 6.3$ J g^{-1}) by differential scanning calorimetry.